PHYSICAL REVIEW D VOLUME 48, NUMBER 9 1 NOVEMBER 1993

Two-body Dirac equation and Regge trajectories

C. Semay* and R. Ceuleneer†
Université de Mons-Hainaut, 19 Avenue Maistriau, B-7000 Mons, Belgium
(Received 21 December 1992)

The spin-triplet spectra of light and heavy neutral mesons are studied in the framework of a free two-body Dirac equation supplemented by a linear scalar confinement interaction. The theoretical Regge trajectories of this model are compared with those of a nonrelativistic model and with the experimental data. Several confinement mechanisms usable for the two-body Dirac equation are presented and the connection with the two-body Klein-Gordon equation is discussed.

PACS number(s): 11.10.Qr, 12.40.Qq

I. INTRODUCTION

The two-body Dirac equation is the most obvious way that makes possible a full spinor treatment of the two fermions. This equation, which is an equal-time relativistic equation, is not fully covariant; nevertheless it exhibits several desirable features, such as good symmetry properties and a correct nonrelativistic limit.

Brayshaw has used such a formalism to study $q\bar{q}$ systems [1]. In his Hamiltonian, the confinement is mainly provided by a cutoff of the wave function at a fixed interquark separation, and the short-range potential is given by the Breit interaction. This model describes quite well the spectra of all mesons with a small number of parameters (two times less than the number required in the semirelativistic model developed by Godfrey and Isgur [2]). However, three major problems remain. First, the Regge trajectories of light mesons are not well described owing to the choice of the confinement mechanism. Second, the Breit interaction fails to reproduce the observed π and K masses; an *ad hoc* contact interaction is introduced to overcome this drawback. Third, it is not possible to describe the mesons η and η' without adding an appropriate mixing procedure with supplementary parameters.

On the other hand, Blask *et al.* [3] have developed a nonrelativistic quark model which describes quite well all mesons, including η and η' states, and baryons composed of u, d, or s quarks. The long-range part of their interaction is a linear confinement potential. The short-range part is not deduced, as usual, from the nonrelativistic reduction of the one-gluon exchange, but is a pairing force stemming from a nonrelativistic limit of instanton effects which acts only on quark-antiquark states with zero spin and orbital angular momentum. A quarkonium which does not contain these configurations is then only submitted to a confinement potential. The weak points of this model are, first, the fact that masses of some mesons are appreciably overestimated, and second, the fact that the Regge trajectories are not well reproduced owing to the choice of a linear confinement, which can be shown, in the large angular momentum limit, by simple dimension arguments [4]. It is worth noting that the pairing force is quite similar to the contact interaction introduced in the model of Brayshaw in that they are both attractive and in that they contribute mainly on the 0^{-+} configuration.

It might be interesting to use the interaction proposed by Blask *et al.* in a relativistic calculation of light meson spectra. In this preliminary work, our purpose is to study the Regge trajectories of the spin-triplet light mesons within the two-body Dirac formalism. According to the model of Blask *et al.*, the quark-antiquark interaction for such mesons is reduced to a confinement potential. Using the confinement interaction of Ref. [5] we have calculated the energy spectrum and the root-mean-square interparticle distance of the spin-triplet mesons by solving numerically the radial equations resulting from the angular momentum decomposition proposed by Brayshaw [1,6]. Actually, for the natural parity spin-triplet states, these equations reduce exactly to a two-body Klein-Gordon equation with masses depending upon the interparticle distance; for the unnatural parity spin-triplet states this is almost the case, as the Dirac spectrum differs from its Klein-Gordon counterpart by less than 2%. For other observables, namely the interparticle distance, the difference between the Dirac and the Klein-Gordon equations is significantly larger.

Our paper is organized as follows. Section II is devoted to the presentation of our model. In that section, several confinement mechanisms usable for the two-body Dirac equation are discussed. The results are analyzed in the third section where they are compared, among others, with the results of the nonrelativistic model of Ref. [7] and the fully covariant treatment of Ref. [8]. Concluding remarks are presented in Sec. IV.

II. MODEL HAMILTONIAN

We study the spin-triplet mesons using a two-body Dirac Hamiltonian given, in the center-of-mass frame, by ($\hbar = c = 1$)

*Electronic address (bitnet): SSEMAY@BMSUEM11
†Electronic address (bitnet): SCEULE@BMSUEM11

$$H=(\boldsymbol{\alpha}_1-\boldsymbol{\alpha}_2)\mathbf{p}+\beta_1 m_1+\beta_2 m_2+\tfrac{1}{2}(\beta_1+\beta_2)\lambda r , \tag{1}$$

where $\mathbf{p}=-i\nabla$ is the conjugate momentum of the variable $\mathbf{r}=\mathbf{r}_1-\mathbf{r}_2$. For such states, the quark-antiquark interaction proposed in Ref. [3] is restricted to a confinement potential that we choose equal to $(\beta_1+\beta_2)\lambda r/2$ as in Ref. [5]. This effective interaction is scalar in order to confine the particles, and the radial form factor is proportional to the interquark distance $r=|\mathbf{r}|$, as it is required to obtain linear Regge trajectories [6,9–11].

We mention here some results obtained in a previous paper [6]. The radial equation for natural parity ($l=J$) is

$$\phi''+\left[\frac{E_1E_2}{\epsilon_1\epsilon_2}-\frac{J(J+1)}{r^2}\right]\phi=0 , \tag{2}$$

where

$$E_1=E-m_1-m_2-\lambda r,\quad E_2=E-m_1+m_2$$

and (3)

$$\epsilon_1=\frac{2E}{E+m_1-m_2},\quad \epsilon_2=\frac{2E}{E+m_1+m_2+\lambda r} ,$$

a prime denoting a derivation with respect to r. The corresponding spinor eigenstates are given by [12]

$$\psi=\frac{\mathcal{N}}{r}\begin{bmatrix} \dfrac{E+m_1+m_2+\lambda r}{2E}\phi|1;J1JJ_z\rangle \\ \dfrac{1}{E-m_1+m_2}\phi'|2;J1JJ_z\rangle+\dfrac{\sqrt{J(J+1)}}{E-m_1+m_2}\dfrac{1}{r}\phi|2;J0JJ_z\rangle \\ -\dfrac{1}{E+m_1-m_2}\phi'|3;J1JJ_z\rangle+\dfrac{\sqrt{J(J+1)}}{E+m_1-m_2}\dfrac{1}{r}\phi|3;J0JJ_z\rangle \\ -\dfrac{E-m_1-m_2-\lambda r}{2E}\phi|4;J1JJ_z\rangle \end{bmatrix} , \tag{4}$$

where $\mathcal{N}$ is a normalization factor and $|i;lsJJ_z\rangle$ are angular basis states defined in Ref. [6]. A more explicit form of Eq. (2) is

$$\phi''+\left[\frac{[E^2-(m_1+m_2+\lambda r)^2][E^2-(m_1-m_2)^2]}{4E^2}-\frac{l(l+1)}{r^2}\right]\phi=0 . \tag{5}$$

Note that this equation is also the radial equation corresponding to the Klein-Gordon equation of two particles with linear radially dependent masses [13]:

$$\left[\mathbf{p}^2+\frac{S_1^2+S_2^2}{2}-\frac{E^2}{4}-\frac{(S_1^2-S_2^2)^2}{4E^2}\right]\psi_{\mathrm{KG}}(\mathbf{r})=0 \quad \text{with } S_i=m_i+\tfrac{1}{2}\lambda r . \tag{6}$$

For the unnatural parity ($l=J\pm1$) spin-triplet states, the radial equations are

$$f_1'-\frac{J}{r}f_1-A^+f_2+Bg_2=0,\quad f_2'+\frac{J}{r}f_2+\frac{E_1}{\epsilon_2}f_1=0,\quad g_1'+\frac{J+1}{r}g_1-A^-g_2+Bf_2=0,\quad g_2'-\frac{J+1}{r}g_2+\frac{E_1}{\epsilon_2}g_1=0 ,$$

with (7)

$$A^{\pm}=\frac{E_2}{\epsilon_1}\pm2\sqrt{J(J+1)}B,\quad B=\frac{2\sqrt{J(J+1)}E_4'}{(2J+1)rE_4^2},\quad E_4=E+m_1+m_2+\lambda r .$$

When B is identically zero, equations containing f_1 and f_2 decouple from those containing g_1 and g_2. They give identical results and thus l becomes a good quantum number. Equations (7) reduce then to the Eq. (5), but with ϕ replaced by f_1 or g_1, and the corresponding spinor-eigenstates are given by [12]

$$\psi=\frac{\mathcal{N}}{r}\begin{bmatrix} \dfrac{E+m_1+m_2+\lambda r}{2E}\phi|1;J\pm11JJ_z\rangle \\ \dfrac{1}{E-m_1+m_2}\left[\phi'\pm\left[J+\dfrac{1\pm1}{2}\right]\dfrac{1}{r}\phi\right]|2;J\pm11JJ_z\rangle \\ -\dfrac{1}{E+m_1-m_2}\left[\phi'\pm\left[J+\dfrac{1\pm1}{2}\right]\dfrac{1}{r}\phi\right]|3;J\pm11JJ_z\rangle \\ -\dfrac{E-m_1-m_2-\lambda r}{2E}\phi|4;J\pm11JJ_z\rangle \end{bmatrix} , \tag{8}$$

where ϕ stands for f_1 or g_1. A numerical analysis shows that the difference between the eigenvalues of Eqs. (7) and those of Eq. (5) is less than 2% for the ground state and decreases rapidly when eigenvalues increase [6]. Thus as far as the energy spectrum is concerned, the Dirac equations and its Klein-Gordon counterpart lead, for the interaction considered in the present work, to very similar spectra.

We have reported elsewhere [6,12] exact and approximate analytical solutions of Eq. (5)

$$m_1=m_2=0, \quad E=\sqrt{2\lambda(4v+2l+3)} \;, \tag{9}$$

$$m_1=0, \quad m_2 \gg \sqrt{\lambda}, \quad E \approx m_2+\sqrt{\lambda}[z(v,l)]^{3/4} \;, \tag{10}$$

$$m_1,m_2 \gg \sqrt{\lambda}, \quad E \approx m_1+m_2+\left[\frac{(m_1+m_2)\lambda^2}{2m_1m_2}\right]^{1/3} z(v,l) \;, \tag{11}$$

where $z(v,l)$ is the solution of the dimensionless equation

$$\left[\frac{d^2}{dx^2}-\frac{l(l+1)}{x^2}-x+z(v,l)\right]w(x)=0 \tag{12}$$

and v is the principal quantum number $(0,1,\ldots)$. Approximate analytical formulas for the quantity $z(v,l)$ have been obtained in Refs. [7,12]. There it is shown that

$$\lim_{l\to\infty} z(v,l) \propto l^{2/3} \;. \tag{13}$$

Thus according to Eqs. (9) and (10), the quantity $[E-m_1-m_2]^2$ is asymptotically proportional to l when one of the quarks is very light.

The mass of quarks n (n denoting u or d) is generally assumed to be very small in relativistic models [1,14,15]. Taking $m_n=0$, Eq. (9) shows that the squared energy of the two quarks is proportional to l, which corresponds to linear Regge trajectories. The best way to reproduce the experimental masses is to rescale the entire spectrum assuming that the masses M of the mesons are expressed by the relation

$$M^2=E^2-C^2 \;, \tag{14}$$

where E is an eigenvalue of the Hamiltonian (1) and C is a constant energy. This constant can be interpreted as a renormalization of the vacuum energy [3]. It has been suggested that the confinement potential has a complex Lorentz structure [16]. It is thus possible that the relation (14) used to shift the spectra appears as a means to simulate approximately the effects of this structure. The parameters λ and C are chosen in order to reproduce the lowest Regge trajectory of the ρ family. The mass of the quark s is taken to reproduce the mass of the ϕ since this meson is practically a pure $s\bar{s}$ state. The values of the four parameters of our model are given in Table I. Note that, although the quarks considered in this model are effective quarks, the quark masses found are compatible with the values generally assumed for the current quark masses [17]. Moreover, in nonrelativistic quarkonium models, a good agreement between theory and experiment is generally obtained by using a negative constant potential whose absolute value is quite similar to the value of the parameter C [3,7,18].

TABLE I. Parameter values of our model in GeV.

$\sqrt{\lambda}=0.535$	$m_n=0$
$C=1.060$	$m_s=0.118$

Though the lowest Regge trajectory of the ρ family can be reproduced with nonvanishing masses for the n quarks, a better agreement with experiment is achieved with $m_n=0$. According to formula (14), the squared masses of mesons can be written

$$M^2(v,l)=\lambda\epsilon^2(v,l)-C^2 \;, \tag{15}$$

where ϵ is an eigenvalue of the dimensionless version of Hamiltonian (1):

$$(\boldsymbol{\alpha}_1-\boldsymbol{\alpha}_2)\mathbf{q}+\beta_1\kappa_1+\beta_2\kappa_2+\tfrac{1}{2}(\beta_1+\beta_2)x \tag{16}$$

with

$$x=\sqrt{\lambda}r, \quad \mathbf{q}=\mathbf{p}/\sqrt{\lambda}, \quad \kappa_i=m_i/\sqrt{\lambda} \;.$$

The quantities

$$R(v,l)=\frac{M^2(v,l)-M^2(0,0)}{M^2(0,1)-M^2(0,0)}=\frac{\epsilon^2(v,l)-\epsilon^2(0,0)}{\epsilon^2(0,1)-\epsilon^2(0,0)} \tag{17}$$

depend only on the dimensionless masses κ_1 and κ_2. For the lowest Regge trajectory of the family of ρ mesons, we have $\kappa_1=\kappa_2=\kappa=m_n/\sqrt{\lambda}$, and the two lowest levels are the $\rho(770)$ $[(v,l)=(0,0)]$ and the $a_2(1320)$ $[(v,l)=(0,1)]$. In Fig. 1, the theoretical values of $R(v,l)$ for the $\rho_3(1690)$ $[(v,l)=(0,2)]$ and $a_4(2040)$ $[(v,l)=(0,3)]$ mesons are compared with their experimental counterparts as a function of κ. It is seen that the best agreement is obtained for small values of κ. Note that,

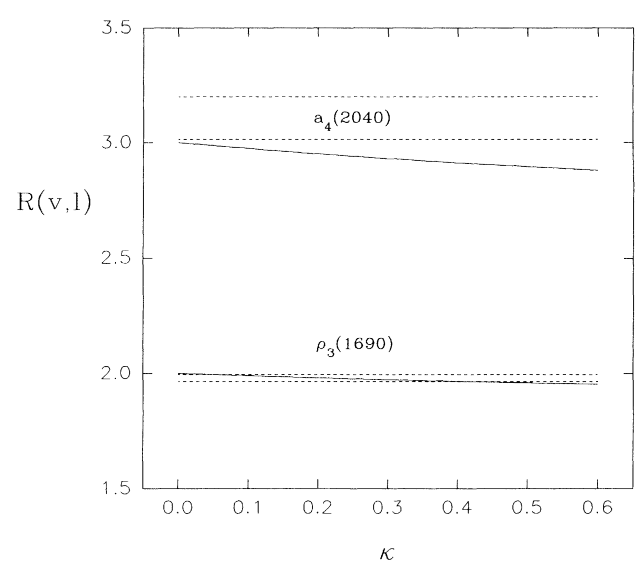

FIG. 1. $R(v,l)$ quantities for the $\rho_3(1690)$ and $a_4(2040)$ mesons (see text). Solid curves are the theoretical results as a function of $\kappa=m_n/\sqrt{\lambda}$. The dashed lines enclose the experimental data with their uncertainties.

according to Eq. (15), it is always possible to fit exactly the theoretical masses of the $\rho(770)$ and $a_2(1320)$ mesons, whatever the value of κ may be. Moreover when κ increases, the value of λ decreases while the value of C increases. For instance, when $\kappa=0.6$, we have $\sqrt{\lambda}=0.467$ GeV, $C=1.345$ GeV, and $m_n=0.280$ GeV.

Other procedures to confine quarks exist within the formalism of the two-body Dirac equation. The interaction $\beta_1\beta_2\lambda r$ can be considered in Hamiltonian (1) instead of $\frac{1}{2}(\beta_1+\beta_2)\lambda r$. Although the expression $\beta_1\beta_2\lambda r$ originates naturally from the reduction of the Bethe-Salpeter equation, we have chosen the operator $\frac{1}{2}(\beta_1+\beta_2)$ because it leads to much more simple radial equations. Moreover, for small quark masses, which is the case for light quarks with relativistic kinematics, and for high energy, which is the case in the study of the Regge trajectories, the spectra associated with these two potentials are quite similar, as illustrated with the following example. According to Eq. (5), the equation for natural parity spin-triplet states with two vanishing masses is

$$\phi''+\left[\frac{E^2-(\lambda r)^2}{4}-\frac{J(J+1)}{r^2}\right]\phi=0 . \tag{18}$$

When $\frac{1}{2}(\beta_1+\beta_2)\lambda r$ is replaced by $\beta_1\beta_2\lambda r$, the corresponding equation is [12]

$$\phi''-\frac{\lambda}{E+\lambda r}\phi'+\left[\frac{E^2-(\lambda r)^2}{4}-\frac{J(J+1)}{r^2}\right]\phi=0 . \tag{19}$$

These two equations give similar results when E increases. For instance, the difference between the ground levels of these two models is around 7%. It drops to less than 2% for the upper level and decreases rapidly when v or l increases. The situation is similar for the unnatural parity spin-triplet states.

Another approach to confine light quarks is to cut off the wave function at a fixed interquark separation r_c [1]. The use of such a mechanism in our model would imply that the spin-triplet quarkonia are eigenstates of the free two-body Dirac Hamiltonian and that the radial functions ϕ, f_1, and g_1 vanish at $r=r_c$. For two massless quarks, the eigenenergies are then given by [1]

$$E=\frac{2}{r_c}k(v,l) , \tag{20}$$

where $k(v,l)$ is the $(v+1)$th zero of the spherical Bessel function of the first kind $j_l(x)$. It is not possible to reproduce the lowest Regge trajectory of the ρ family with formula (20) since [19]

$$\lim_{l\to\infty} k(0,l)\propto l . \tag{21}$$

We have verified that neither rescalings of Eq. (20) such that $M^2=E^2\pm C^2$ or $M=E\pm C$, nor the use of nonmassless quarks, can provide a good fit for this trajectory.

III. RESULTS

From Figs. 2 to 9, we compare our theoretical results with the experimental data and with the results of the nonrelativistic model of Ref. [7], in which the interaction is also reduced to the confinement. The potential of this model, which is fitted to reproduce the Regge trajectories, is given by

$$V(r)=0.431r^{2/3}-1.210 \tag{22}$$

with

$$m_n=0.270 \text{ GeV}, \quad m_s=0.516 \text{ GeV} ,$$

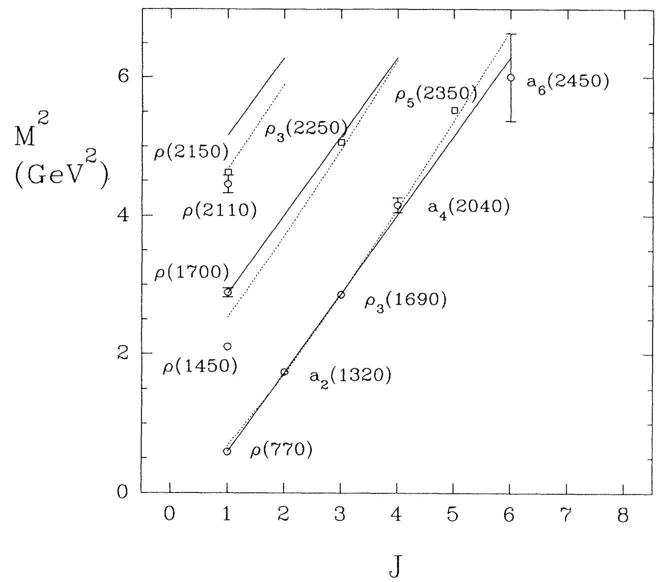

FIG. 2. Mass spectrum for the ρ family $[J=l+1]$ as a function of J. The solid and dotted lines indicate the results of our model and the results of the Fabre model [7], respectively. Experimental values of masses are indicated by a circle; states for which error on mass is unestimated in Ref. [20] are shown by a box.

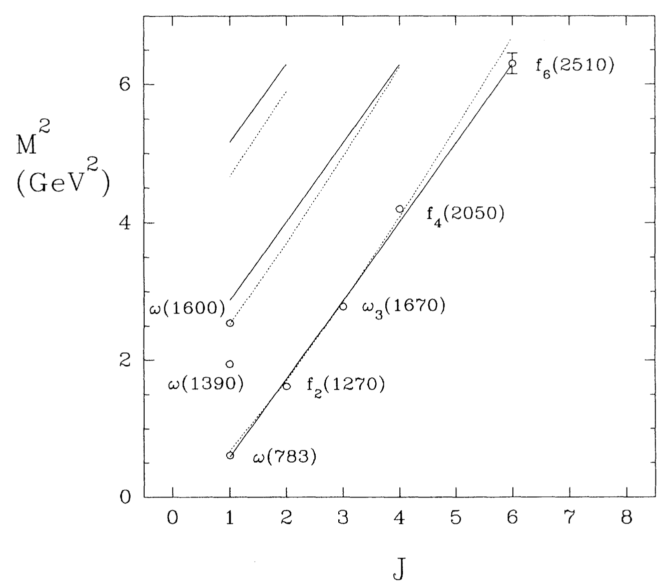

FIG. 3. Same as Fig. 1 for the ω family $[J=l+1]$.

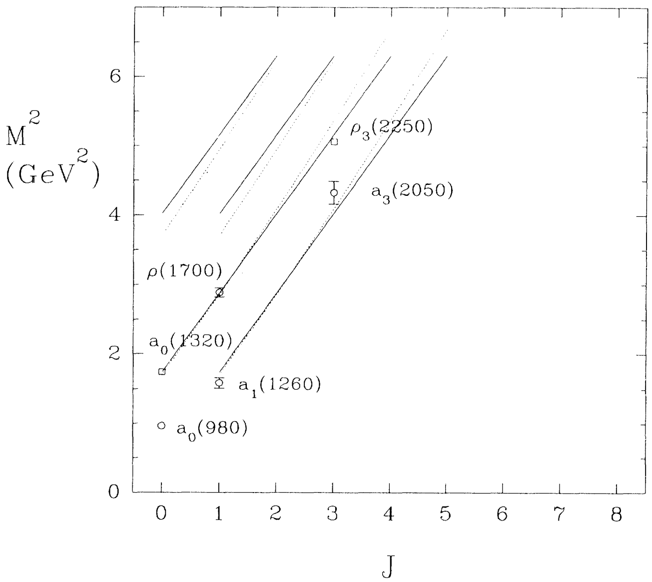

FIG. 4. Same as Fig. 1 for the a_1 family [$J=l$] and the a_0 family [$J=l-1$].

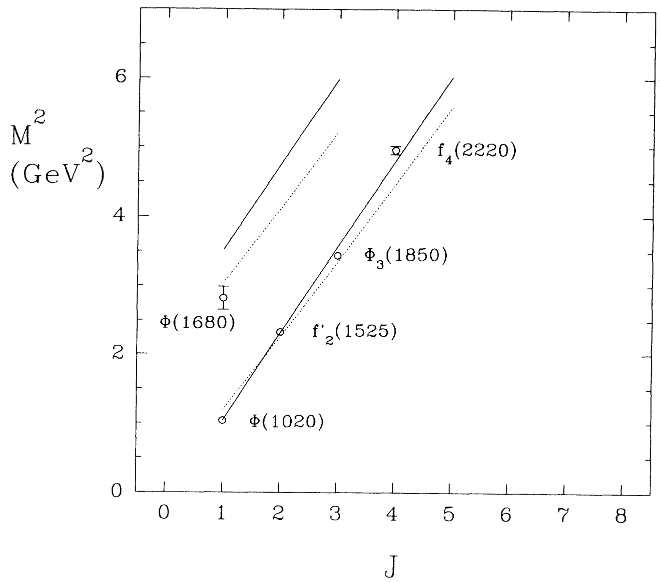

FIG. 5. Same as Fig. 1 for the ϕ family [$J=l+1$].

with V in GeV and distance in GeV^{-1}. The experimental masses are taken from the 1992 compilation of masses of the Particle Data Group [20].

A. Orbital excitations

The parameters m_n, λ, and C are fitted to yield the correct lowest Regge trajectory of the ρ family (see Fig. 2). Since the spin-triplet isoscalar $n\bar{n}$ mesons are nearly degenerated with the spin-triplet isovector mesons, the lowest trajectory of the ω family is also well reproduced (see Fig. 3). Note that though the masses of the isovector mesons are completely fixed by the masses of the states of the ρ family [$J=l+1$], the agreement between the theoretical and experimental masses of the two known members of the a_1 family [$J=l$] is quite satisfactory (see Fig. 4). The situation of the a_0 family [$J=l-1$] is also quite satisfactory provided one assumes that the $a_0(980)$ is not a $q\bar{q}$ state and that the lowest $^3P_0$ state is the resonance $a_0(1320)$. Actually, experimental considerations [20] and theoretical works [21,22] suggest that the $a_0(980)$ meson is a $K\bar{K}$ bound state. In the same way, though the value of m_s is only fixed by the mass of the ϕ meson, the lowest trajectories of the ϕ family and of the K^* family [$J=l+1$] are very well reproduced (see Figs.

TABLE II. Masses in GeV of the ground-state mesons ($1\,^3S_1$) ρ, ω, K^*, and ϕ with their two lowest excitations ($2\,^3S_1$ and $1\,^3D_1$) with the same $J^{P(C)}=1^{-(-)}$ quantum numbers, for various models, compared with the experimental scheme proposed by Ref. [20]. Each model is indicated by the first author and the number of the corresponding reference. The results of Ref. [8] are taken from the best global fit obtained by the authors. According to Ref. [20], the two mesons indicated by an asterisk could invert their places.

Meson		Expt. [20]	Our model	Fabre [7]	Bhaduri [18]	Blask [3]	Brayshaw [1]	Godfrey [2]	Crater [8]
ρ	$1\,^3S_1$	0.770	0.769	0.822	0.777	0.770	0.776	0.770	0.889
	$2\,^3S_1$	1.450	1.696	1.591	1.614	1.565	1.824	1.450	1.746
	$1\,^3D_1$	1.700	1.696	1.690	1.678	1.634	1.593	1.660	1.795
ω	$1\,^3S_1$	0.783	0.769	0.822	0.777	0.770	0.776	0.780	0.889
	$2\,^3S_1$	1.390	1.696	1.591	1.614	1.565	1.824	1.460	1.746
	$1\,^3D_1$	1.600	1.696	1.690	1.678	1.634	1.593	1.660	1.795
K^*	$1\,^3S_1$	0.892	0.900	0.970	0.905	0.924	0.905	0.900	0.911
	$2\,^3S_1$	1.410*	1.788	1.688	1.694	1.656	1.872	1.580	1.761
	$1\,^3D_1$	1.680*	1.794	1.781	1.774	1.723	1.690	1.780	1.809
ϕ	$1\,^3S_1$	1.020	1.019	1.091	1.017	1.061	1.022	1.020	0.975
	$2\,^3S_1$	1.680	1.878	1.745	1.743	1.714	1.925	1.690	1.793
	$1\,^3D_1$		1.888	1.829	1.834	1.775	1.778	1.880	1.842

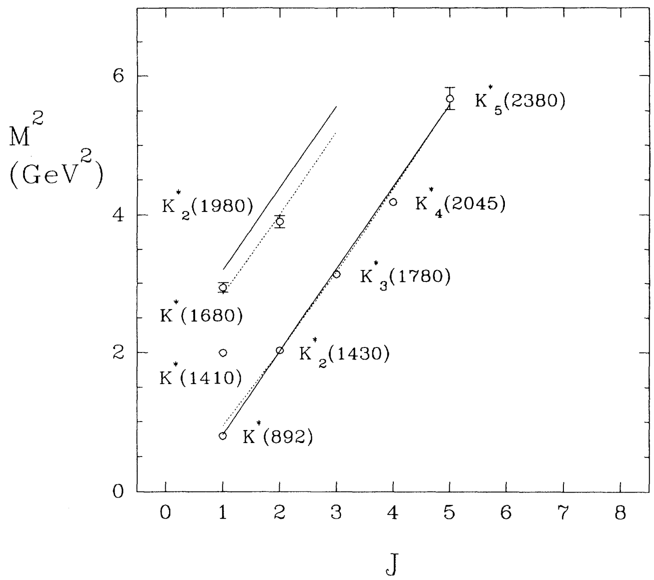

FIG. 6. Same as Fig. 1 for the K^* family $[J=l+1]$.

5 and 6).

Only the lowest members of the $J=l$ and $J=l-1$ families of isoscalar and isodoublet mesons are known [20]. As the spin-triplet states belonging to a l multiplet are experimentally nearly degenerated, our model yields also good masses for these mesons.

The results reported in Ref. [7] for the lowest Regge trajectory compare quite well with our results. Nevertheless, it can be seen from Table II that our predictions concerning the low-lying state of each family are better than those of Ref. [7]. Actually, both nonrelativistic and ultrarelativistic approaches can yield a good description of the light meson spectra provided an appropriate effective confinement potential is used [11,23].

B. Radial excitations

It appears from Figs. 2 to 6 that our model seems to provide a better description of the orbital excitations of light mesons than the radial excitations. In Table II, we compare, for various potential models, the ground states of several $1^{-(-)}$ mesons and their two lowest excitations with the same $J^{P(C)}$ quantum numbers. The approaches of Brayshaw [1], Blask *et al.* [3], and Fabre [7] have been described above. The model of Bhaduri *et al.* [18] is a nonrelativistic one in which the long-range part of the potential is a linear confinement and the short-range part is the Coulomb interaction supplemented by the color hyperfine term. This simple model is mainly fitted for charmonium and bottomium sectors but gives acceptable masses for mesons containing lighter quarks. On the other hand, the semirelativistic model of Godfrey and Isgur [2] provides a better global description of all meson states but their interaction which contains a great number of parameters is very complex. Another good global fit of all mesons has been obtained within the fully covariant formalism developed by Crater and Van Alstine [8]; the potentials used by these authors contain only one or two parameters.

In Ref. [20] the $\rho(1450)$ is identified with the first radial excitation ($2\,^3S_1$ state) of the $\rho(770)$ while the $\rho(1700)$ is considered as its D-wave excitation with the same J^{PC} quantum numbers ($1\,^3D_1$ state). As it can be seen from Table II, the $2\,^3S_1$ state and the $1\,^3D_1$ state are characterized by the same mass of 1.696 GeV in our model. Consequently, our calculations are not in agreement with the experimental data. Of course, it is quite possible that our model cannot correctly describe the radial excitations. However, it is also possible that the $\rho(1700)$ could be a superposition of two nearly degenerate 1^{--} states, one of which, the $2\,^3S_1$ state, belongs to the ρ family (see Fig. 2) and the other, the $1\,^3D_1$ state, can be interpreted as the first orbital excitation of the $1\,^3P_0$ state, which is assumed here to be the $a_0(1320)$ meson (see Fig. 4). In that case the $\rho(1450)$ cannot be considered an ordinary $q\bar{q}$ meson. The models of Crater and Brayshaw also favor this hypothesis, contrary to the model of Godfrey and Isgur. The theoretical mass yielded by the other models is around 1.6 GeV. It is worth noting that the experimental situation could be more complicated with, for instance, mixing of $\rho(1450)$ and $\rho(1700)$ with $q^2\bar{q}^2$ states, as suggested in Ref. [24]. Such mixing could in principle explain the hadronic shift of $q\bar{q}$ states and the observed branching ratios in the vector meson sector [25,26]. Note that a similar problem exists in the baryon sector. The two lowest excited states of the nucleon are the $N(1440)$ and the $N(1710)$. A lot of potential models (see, for instance, Ref. [27]) predict the first radial excitation of the nucleon near 1.7 GeV, suggesting that the Roper resonance could be a non-q^3 state and that the $N(1710)$ could be the first radial excitation of the nucleon. Even the models which predict a lower mass for the first excitation of the nucleon cannot reproduce correctly the mass of the Roper resonance (see for instance Ref. [28]).

The internal structure of the $\rho_3(2250)$ is also difficult to determine. Owing to the exact degeneracy of $n\bar{n}$ states in our model [see Eq. (9)], this meson could be identified as a $2\,^3D_3$ state or as a $1\,^3G_3$ state (see Figs. 2 and 4).

Since the mesons of ρ and ω families are nearly degenerate, the problems concerning the identification of their radial excitations are the same in both cases. Moreover, in the isoscalar sector, a large number of f_2 resonances exist but are not predicted by quark models. All these states, whose accurate identification is tricky, could be exotic multiquarks or glueball systems [29].

According to Ref. [20], the identification of the two lowest 1^- excitations of the K^* is also difficult. The mesons $K^*(1410)$ and $K^*(1680)$ are both possible candidates for these excitations. The mass of the lowest excited state of each model considered in Table II is much larger than 1.4 GeV. For the ϕ meson, only the $\phi(1680)$ excitation is known and it is identified with the first radial excitation. Except for the model of Godfrey and Isgur, the other models, including ours, predict an appreciable larger mass for this first radial excitation.

The predictions of our model concerning the radial excitations of light mesons are not in agreement with the experimental data. Some mesons, namely $\rho(1450)$,

TABLE III. Masses in GeV of heavy mesons in our model and in the Fabre model [7]. Underlined masses are those used to determine the values of m_c and m_b.

	Our model		Fabre [7]	
m_c	1.194	1.143	1.681	1.647
$J/\psi(3097)$	3.097	2.998	3.097	3.034
$D^*(2010)$	2.064	2.010	2.044	2.010
$D_s^*(2110)$	2.145	2.092	2.128	2.096
m_b	4.456	4.383	4.975	4.999
$\Upsilon(9460)$	9.460	9.316	9.460	9.507
$B^*(5331)$	5.405	5.331	5.307	5.331

$\omega(1390)$, and $K^*(1410)$, seem to appear as extra states in Figs. 2 to 6. The existence of some $q^2\bar{q}^2$ vector mesons, which could be identified with these states, cannot be excluded [24]. The P-wave $q^2\bar{q}^2$ mesons, which are the lowest states with negative parity, might be good candidates for such resonances. Another, more likely, possibility is that our model, like some others, overestimates masses of the radial excitations of light mesons.

In order to test our model concerning radial excitations, we have calculated such excitations for the J/ψ and the Υ mesons whose experimental radial spectra are well known. The one-gluon exchange potential must certainly contribute to the mass of heavy neutral mesons [3,7]. Nevertheless, we find it interesting to compare the predictions of our model in this sector with those obtained with the potential (22) of the nonrelativistic model

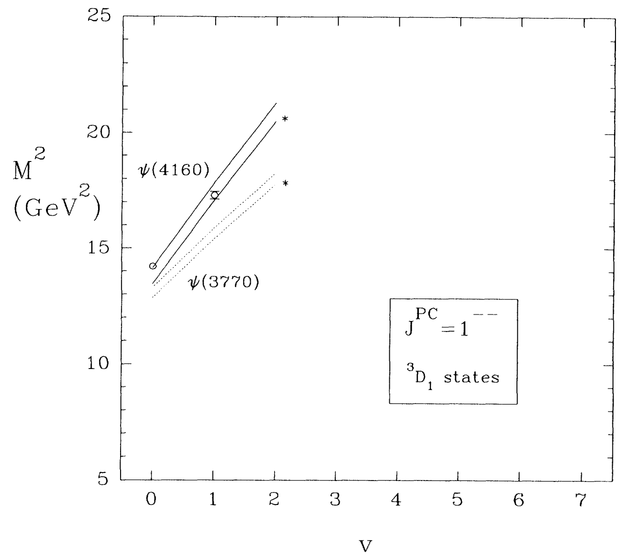

FIG. 8. Same as Fig. 7 for the $^3D_1$ ψ mesons.

of Ref. [7]. Note that for heavy neutral mesons the Hamiltonian (1) is nearly equivalent to a nonrelativistic Hamiltonian with a linear confinement. For both models, the value of m_c (m_b) has been fitted to reproduce either the mass of the J/ψ (Υ) or the mass of the D^* (B^*); the results are given in Table III. We would like to stress that, despite the absence of the one-gluon exchange po-

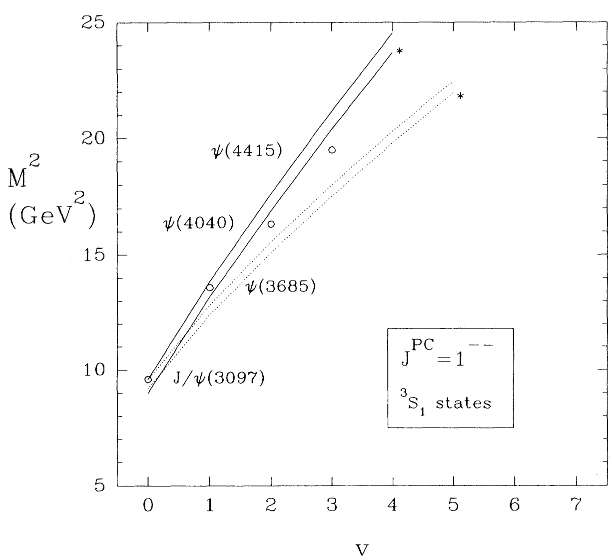

FIG. 7. Mass spectrum for the $^3S_1$ ψ mesons as a function of v. The solid and dotted lines indicate the results of our model and the results of the Fabre model [7], respectively. Experimental values of masses are indicated by a circle. The curves labeled by an asterisk are obtained with a value of m_c fitted to reproduce the D^*. For the other curves, the value of m_c is fitted to reproduce the J/ψ.

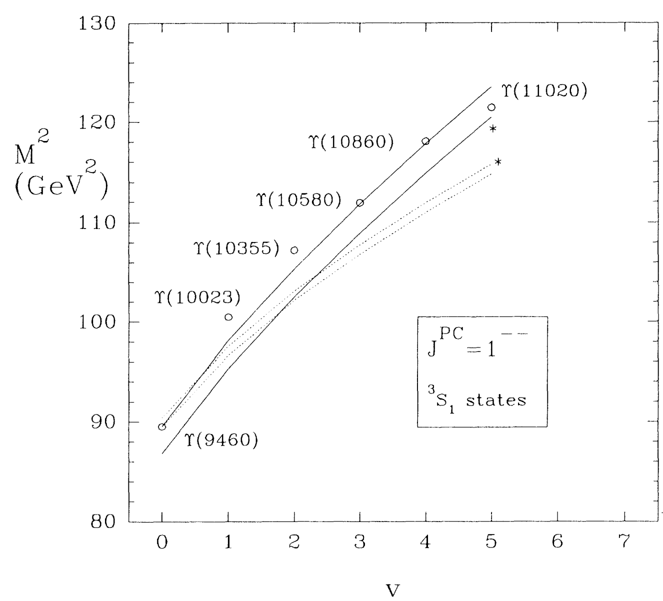

FIG. 9. Mass spectrum for the $^3S_1$ Υ mesons as a function of v. The solid and dotted lines indicate the results of our model and the results of the Fabre model [7], respectively. Experimental values of masses are indicated by a circle. The curves labeled by an asterisk are obtained with a value of m_b fitted to reproduce the B^*. For the other curves, the value of m_b is fitted to reproduce the Υ.

TABLE IV. Expectation values of $\sqrt{\lambda\langle r^2\rangle}$ (see text) for different mesons within our two-body Dirac model and within an equivalent two-body Klein-Gordon model.

Meson	$\sqrt{\lambda\langle r^2\rangle}$ Dirac	KG
$\rho(770)$	2.00	1.73
$a_2(1320)$	2.45	2.24
$K^*(892)$	1.93	1.69
$\phi(1020)$	1.86	1.64

tential, our predictions for radial excitations appear acceptable and, moreover, are in better agreement with the data than the predictions of the nonrelativistic model (see Figs. 7 to 9). The results of the nonrelativistic model can be improved by the introduction of a Coulomb-like term but, even in this case, it is impossible to adjust simultaneously the light and heavy meson spectra with a $r^{2/3}$ confinement potential [7]. Consequently, in the nonrelativistic models, a $r^{2/3}$ confinement is necessary to reproduce the linear Regge trajectories of light mesons but a linear confinement seems preferable to describe the heavy meson spectra. The advantage of the relativistic models in that a linear confinement potential works well both for light and heavy mesons.

As mentioned above, the spectra resulting from (1) and (6) are very similar, but this is obviously not the case for the corresponding eigenfunctions. To illustrate this point, we have calculated the root-mean-square dimensionless interparticle distance between quarks $\sqrt{\lambda\langle r^2\rangle}$ for different mesons with the solutions of Hamiltonian (1) and those of Eq. (6). As we can see in Table IV, the results are significantly different, despite the fact that the operator r^2 is spin independent. The difference can exceed 10%, whereas the difference between the eigenenergies is always less than 2%.

IV. CONCLUDING REMARKS

The use of quark potential models is relevant in the adiabatic limit, which implies that the typical time scale of quark fields T_q is much larger than the typical time scale of the gluonic fields T_g. T_q is defined as the period of a quark motion around the classical orbit [30]. It can be evaluated by the relation $T_q \approx 2\pi R_q/v_q$, R_q being the radius of the quark orbit given by $\sqrt{\langle r^2\rangle}/2$ and v_q the speed of the quark. In our model, for the ground state of two massless quarks, we have $v_q \approx c = 1$ and $\sqrt{\langle r^2\rangle} = 2/\sqrt{\lambda}$ (see Table IV). Consequently we find $T_q \approx 12\ \text{GeV}^{-1}$. We obtain similar values of T_q for the nonrelativistic models of Blask *et al.* and Fabre. Note that in these models, v_q, which is given by the relation $\sqrt{\langle \mathbf{p}^2/m^2\rangle}$, is around 1, making the interpretation of the parameters of these models questionable. This general problem of the nonrelativistic approach is discussed in Refs. [13,31]. T_g, which is the gluonic vacuum correlation time, is expected to be less than $3\ \text{GeV}^{-1}$ [32]. Consequently, it seems reasonable to assume, as well for nonrelativistic than for ultrarelativistic models, that the quarks move adiabatically and that the potential approach is relevant.

We have calculated the masses of the spin-triplet light mesons in the two-body Dirac formalism, assuming that the interaction is reduced to a confinement potential given by linear radially dependent masses. In our model, which contains only two parameters other than quark masses, the lowest Regge trajectories are well reproduced. The agreement between theory and experiment is poorer for upper trajectories. Note that the results of the fully covariant model of Ref. [8] are very similar to our results but that the Regge trajectories are better reproduced within our model. Despite the absence of a Coulomb-type potential in our calculation, our description of the radial excitations of the $c\bar{c}$ and $b\bar{b}$ mesons appears acceptable.

ACKNOWLEDGMENTS

We would like to thank Dr. B. Silvestre-Brac, Dr. B. Desplanques, and Professor I. M. Narodetskii for stimulating discussions.

[1] D. D. Brayshaw, Phys. Rev. D **36**, 1465 (1987).
[2] S. Godfrey and N. Isgur, Phys. Rev. D **32**, 189 (1985).
[3] W. H. Blask *et al.*, Z. Phys. A **337**, 327 (1990).
[4] S. Godfrey, Phys. Rev. D **31**, 2375 (1985).
[5] P. Leal Ferreira, Phys. Rev. D **38**, 2648 (1988).
[6] R. Ceuleneer, P. Legros, and C. Semay, in *Proceedings of the European Workshop on Hadronic Physics with Electrons Beyond 10 GeV*, Dourdan, France, 1990, edited by B. Frois and J.-F. Mathiot [Nucl. Phys. **A532**, 395c (1991)].
[7] M. Fabre de la Ripelle, Phys. Lett. B **205**, 97 (1988).
[8] H. W. Crater and P. Van Alstine, Phys. Rev. D **37**, 1982 (1988).
[9] C. Goebel, D. LaCourse, and M. G. Olsson, Phys. Rev. D **41**, 2917 (1990).
[10] W. Lucha, H. Rupprecht, and F. F. Schöberl, Phys. Lett. B **261**, 504 (1991).
[11] W. Lucha and F. F. Schöberl, Z. Phys. C **53**, 83 (1992).
[12] C. Semay, R. Ceuleneer, and B. Silvestre-Brac, J. Math. Phys. **34**, 2215 (1993).
[13] D. B. Lichtenberg, Int. J. Mod. Phys. A **2**, 1669 (1987).
[14] J. L. Basdevant and S. Boukraa, Z. Phys. C **28**, 413 (1985).
[15] B. Rosenstein, Phys. Rev. D **33**, 813 (1986).
[16] Junchen Su, Yubing Dong, and Shishu Wu, J. Phys. G **18**, 1347 (1992).
[17] G. A. Miller, B. M. K. Nefkens, and I. Slaus, Phys. Rep. **194**, 1 (1990).
[18] R. K. Bhaduri, L. E. Cohler, and Y. Nogami, Il Nuovo Cimento **65A**, 376 (1981).
[19] *Handbook of Mathematical Functions*, edited by M. Abramowitz and I. A. Stegun (Dover, New York, 1964), p. 371.
[20] Particle Data Group, K. Hikasa *et al.*, Phys. Rev. D **45**, S1 (1992).
[21] J. Weinstein and N. Isgur, Phys. Rev. D **41**, 2236 (1990).
[22] B. Silvestre-Brac and C. Semay, Z. Phys. C **57**, 273 (1993).
[23] C. Semay and B. Silvestre-Brac, Phys. Rev. D **46**, 5177

(1992).
[24] Yu. S. Kalashnikova, Yad. Fiz. **55**, 514 (1992) [Sov. J. Nucl. Phys. **55**, 286 (1992)].
[25] A. Donachie and B. Mizzaie, Z. Phys. C **33**, 407 (1987).
[26] A. B. Clegg and A. Donachie, Z. Phys. C **40**, 313 (1988).
[27] B. Silvestre-Brac and C. Gignoux, Phys. Rev. D **32**, 743 (1985).
[28] S. Capstick and N. Isgur, Phys. Rev. D **34**, 2809 (1986).
[29] M. Poulet, in *Proceedings of LEAP '90,* Stockholm, Sweden, 1990, edited by P. Carlson, A. Kerik, and S. Szilagyi (World Scientific, Singapore, 1991), p. 304.
[30] I. M. Narodetskii, Few-Body Systems, Suppl. 6, 148 (1992).
[31] W. Lucha, F. F. Schöberl, and D. Gromes, Phys. Rep. **200**, 127 (1991).
[32] Yu. A. Simonov, Nucl. Phys. **B324**, 67 (1989).